

---

# Wheel Rail Wear Prediction and Dynamic Performance Analysis of Linear Metro

---

Ding Feng, Long Chen\*, Yanxia Yu  
and Yunfeng Zeng

*CRRC Dalian Locomotive & Rolling Stock Co., Ltd., China*

*E-mail: duxiaoyang@dl-laike.com*

*\*Corresponding Author*

Received 08 June 2022; Accepted 14 July 2022;  
Publication 13 August 2022

## **Abstract**

In order to improve the safety of linear motor metro operation, the wheel rail wear prediction and dynamic performance analysis of linear motor metro are carried out. Firstly, the working principle and evolution process of the linear motor are analyzed, and the traveling wave magnetic field and slip ratio of the linear motor are calculated. Secondly, the friction principle between wheel and rail is analyzed, and the running data of wheel and rail area are collected by MiniProf series profiler. By calculating the wear energy flow density and wear mass flow density of wheel rail contact surface, the relationship between wear coefficient and energy flow density is obtained, and the wheel rail wear area is obtained, so as to complete the prediction of wheel rail wear. Finally, the running resistance of Metro is analyzed, including mechanical resistance and aerodynamic resistance. Combined with the calculation results of Metro kinetic energy and electromagnetic, the position of linear motor is obtained by modal superposition method in the elastic coordinate system, and the dynamic equation of linear motor Metro is constructed to complete

*European Journal of Computational Mechanics, Vol. 31.2, 217–238.*

doi: 10.13052/ejcm2642-2085.3123

© 2022 River Publishers

the dynamic performance analysis of Metro. The experimental results show that this research method can accurately predict the wear of linear motor metro, and can study the running stability of Metro from the two aspects of horizontal stability and derailment coefficient.

**Keywords:** Linear motor, metro wheel rail, wear prediction, dynamic performance.

## 1 Introduction

With the continuous development of urban traffic, subway has gradually become an effective means of transportation, which greatly meets the daily travel needs of urban residents with its huge carrying advantages [1]. With the development of computational power technology, a kind of linear motor has been developed on the basis of rotating motor. Compared with rotating motor, linear motor has the characteristics of sufficient power and strong climbing ability. The climbing gradient of linear motor Metro can reach 60‰~80‰, which can meet the needs of metro operation in cities with complex terrain [2–4]. However, with the increase of running mileage, the Metro wheel rail of linear motor will be subject to certain wear. If the wear is serious, it will affect the safety of metro operation. Therefore, it is very necessary to predict the wear degree of Metro wheel rail of linear motor and analyze the dynamic performance under wear [5, 6].

Reference [7] in order to study the driving performance of linear motor Metro in curve sections, a dynamic model of Metro wheel rail is built. With the support of the model, the relationship between the traction speed and time slot of the motor under the action of vertical electromagnetic force is studied. The dynamic response performance of linear metro is analyzed by changing the electromagnetic force, curve radius and track smoothness. Reference [8] in order to study the wear of Metro wheel and rail, the multi-body dynamics software is used to build the Metro dynamics simulation model to analyze the dynamic performance of the wheel in contact with chn60 rail, and the surface fatigue index is used to analyze the fatigue characteristics Of the wheel and rail. Reference [9] takes the metro with different types of motors as the research object to study the wheel rail wear and dynamic performance. Firstly, the evolution law of Metro wheel rail wear, wear area and wear rate is analyzed. Secondly, the wear amount in different states is obtained by changing the stability and stability of metro operation. Finally, the wheel rail

structure characteristic model and dynamic model are constructed to reveal the dynamic characteristics of Metro.

In order to improve the running safety of linear metro, a method of wheel rail wear prediction and dynamic performance analysis for linear metro is proposed.

## 2 Structure Analysis of Linear Metro

The basis of linear motor is still rotating motor, so the working principle of linear motor is basically the same as that of rotating motor. In terms of electromagnetic force, the traveling wave magnetic field is generated by the primary coil of both motors. At this time, the induction plate will generate eddy current, which will cut the magnetic field to generate electromagnetic force [10]. In terms of motor structure, the rotating motor can be cut along the radius and expanded to obtain the linear motor. Therefore, the stator and rotor of the rotating motor can be regarded as the primary and secondary of the linear motor respectively. The evolution process of linear motor is shown in Figure 1.

The magnetic field in the linear motor is a traveling wave magnetic field, and the synchronous speed of the magnetic field can be expressed as:

$$v_s = 2\tau f \tag{1}$$

In the formula,  $\tau$  represents the pole distance of linear motor and  $f$  represents the frequency of current [11].

Slip ratio of linear motor can be written as:

$$s = \frac{v_s - v}{v_s} \tag{2}$$

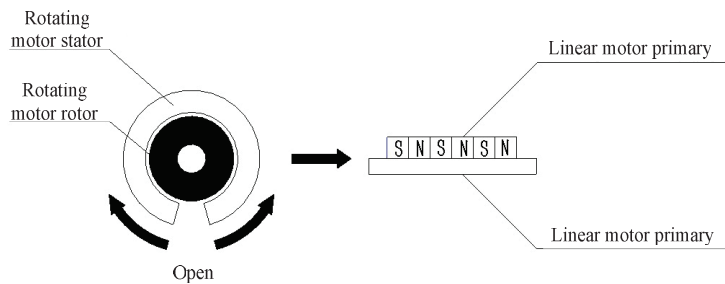
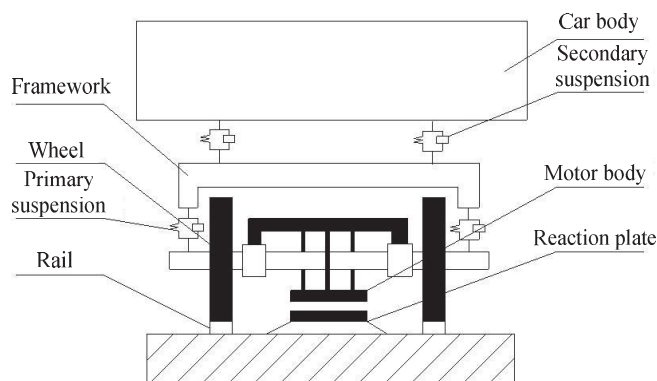


Figure 1 Evolution of linear motor.



**Figure 2** Structure diagram of linear metro.

In the formula,  $v$  represents the moving speed of the secondary in the linear motor.

Compared with the rotary motor metro, there is no gear transmission between the motor and wheel set of the linear motor Metro [12], so the traditional system structure of the whole vehicle is more simplified. The structural diagram of the linear motor Metro is shown in Figure 2.

It can be seen from Figure 2 that the linear metro is mainly composed of primary suspension device, secondary suspension device, car body, bogie, linear motor and wheel set system. Therefore, the wear between wheel set and track is the key content affecting the operation safety of the whole Metro. Therefore, the linear metro wheel rail wear prediction is carried out and the dynamic performance under wheel rail wear is studied [13–15].

### 3 Wheel Rail Wear Prediction of Linear Metro Based on Data Acquisition

Wheels are an important part of the metro. Once serious wear occurs, it will lead to derailment or wheel collapse. Therefore, it is necessary to analyze the failure causes of Metro wheels and strengthen the management of Metro quality [16]. The schematic diagram of abnormal wear of wheel rail tread is shown in Figure 3.

When the linear metro wheel set moves along the track, there is not only a separate rolling motion between the wheel and the rail, but creep and rotation in the contact area between the wheel and the rail. The creep



Figure 3 Abnormal wear of wheel-rail tread.

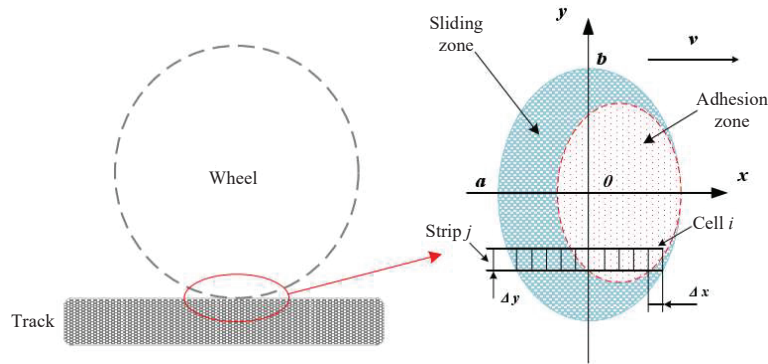


Figure 4 Creep diagram.

motion mainly includes three components: longitudinal, transverse and spin. The creep diagram is shown in Figure 4.

Before the wheel rail wear prediction of linear metro, it is necessary to collect the operation data of the wheel and track area. Using MiniProf series contour measuring instrument for contact measurement can improve the accuracy of data collection and reduce the cost of collection [17, 18]. The measuring device is shown in Figure 5.

Based on the data collected by the measuring device, the wear prediction is calculated. Firstly, the curve deviation function of linear metro is constructed to express the curve deviation:

$$F(X, Y, \alpha) = \sum_{k=1}^n (||d_k||) / n \quad (3)$$

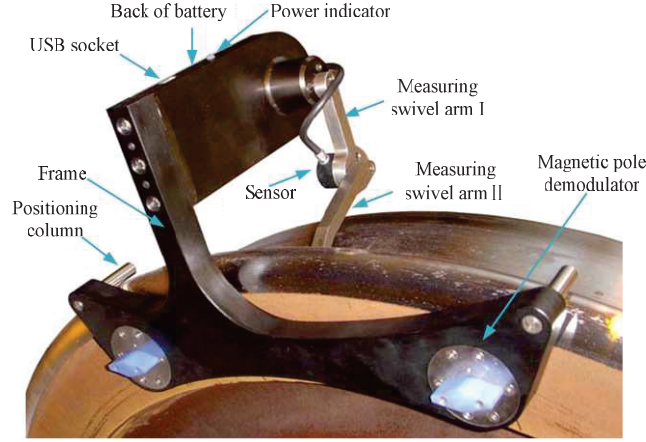


Figure 5 Measuring device.

In the formula,  $X$  represents transverse motion,  $Y$  represents longitudinal motion,  $\alpha$  represents rotation of coordinate origin,  $d_k$  represents distance between adjacent points on the curve before and after wear, and  $n$  represents scattered points after wear [19].

When the volume of linear metro wheel rail wear rubs against the contact surface, the expression of energy and volume dissipated by the relative motion of the two is:

$$V = k_R W \quad (4)$$

In the formula,  $V$  represents the volume of wheel set material,  $k_R$  represents the wear constant of wheel rail, and  $W$  represents the wear work of wheel set material.

The calculation formula of wear energy flow density at one point of wheel rail contact surface is:

$$\dot{E}_d(r_p, t) = \begin{cases} \frac{F_x V_x + F_y V_y + M_z w_z p(r_p, t)}{A(t) \bar{p}(t)}, & r_p \in A(t) \\ 0, & r_p \notin A(t) \end{cases} \quad (5)$$

In the formula,  $(r_p, t)$  represents the coordinate position of the contact point,  $\dot{E}_d$  represents the energy flow density,  $F_x$  and  $F_y$  represent the transverse force and longitudinal force of creep respectively,  $M_z$  represents the torque during creep,  $w_z$  represents the sliding speed during spin,  $\bar{p}(t)$  represents the mean value of wheel rail contact stress, and  $A(t)$  represents the contact area [20].

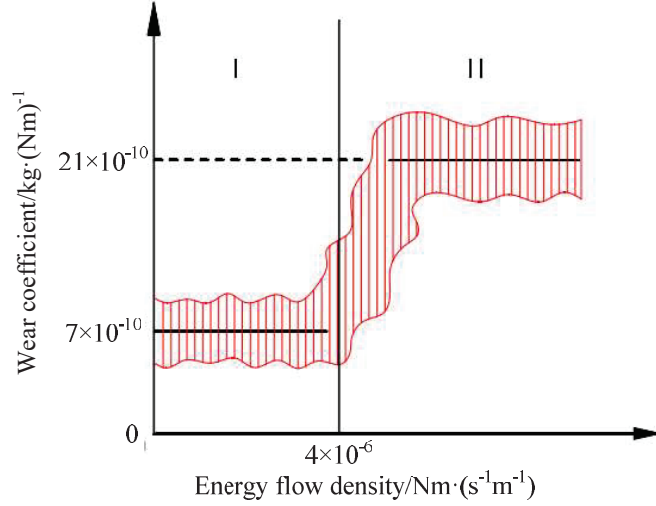


**Figure 6** Energy flow density.

The calculation formula of wheel rail wear mass flow density is:

$$\dot{m}_d(i, j) = k_Z(i, j) \cdot \dot{E}_d(r_p, t) \quad (6)$$

In the formula,  $k_Z$  represents the wear coefficient of wheel rail. According to formula (6), the relationship between wear coefficient and energy flow density can be obtained, as shown in Figure 6.

According to the energy dissipation parameters, the calculation formula of wheel rail wear area is constructed:

$$\delta_p = \begin{cases} \text{I} & \frac{0.25 \vec{T} \cdot \vec{\xi}}{D}, \vec{T} \cdot \vec{\xi} < 100N \\ \text{II} & \frac{25}{D}, 100N \leq \vec{T} \cdot \vec{\xi} \leq 200N \\ \text{III} & \frac{1.19 \vec{T} \cdot \vec{\xi} - 154}{D}, \vec{T} \cdot \vec{\xi} > 200N \end{cases} \quad (7)$$

In the formula,  $\delta_p$  represents the wear area of wheel rail,  $D$  represents the diameter of Metro wheel,  $\vec{T}$  represents the creep force within the contact area, and  $\vec{\xi}$  represents the creep rate.

I, II and III in formula (7) represent light, medium and heavy wear respectively.

#### 4 Dynamic Performance Analysis of Linear Metro Wheel Rail Based on Modal Superposition

After the wheel rail wear prediction of linear metro is completed, the mechanical performance of linear metro under wear is analyzed. In general, the resistance suffered by the subway during operation mainly includes mechanical resistance and aerodynamic resistance. Therefore, the resistance suffered by the linear motor subway is analyzed first [21]. The size of subway resistance is mainly affected by vehicle speed. The expression of subway air resistance is constructed:

$$F_d = \frac{\rho \cdot S_c \cdot v^2 \cdot (C_D + \frac{\lambda}{dl})}{2} \quad (8)$$

In the formula,  $S_c$  represents the cross-sectional area of the subway,  $\rho$  represents the air density,  $v$  represents the running speed of the subway [22],  $C_D$  represents the aerodynamic resistance coefficient,  $\lambda$  represents the hydraulic friction coefficient,  $d$  represents the hydraulic diameter, and  $l$  represents the length of the subway.

The mechanical resistance of linear metro is mainly affected by the extrusion between wheel and rail, so the expression of mechanical resistance can be written as:

$$F_f = \mu \cdot N \quad (9)$$

In the formula,  $\mu$  represents the wheel rail friction coefficient of Metro.

During the operation of linear metro, the system of electromagnetic and mechanical interaction is electromechanical coupling system. In order to analyze the dynamic characteristics of the system [23], it is necessary to comprehensively consider the influence factors of electromagnetic and mechanical. In order to simplify the calculation process, the dynamic equation of electromechanical coupling system is constructed:

$$\begin{cases} \frac{d}{dt} \left( \frac{\partial L}{\partial \dot{e}_k} \right) - \frac{\partial L}{\partial e_k} + \frac{\partial F_w}{\partial \dot{e}_k} = U_k (k = 1, 2, \dots, n) \\ \frac{d}{dt} \left( \frac{\partial L}{\partial \dot{q}_j} \right) - \frac{\partial L}{\partial q_j} + \frac{\partial F_W}{\partial \dot{q}_j} = Q_j (j = 1, 2, \dots, m) \end{cases} \quad (10)$$

In the formula,  $F_w$  represents the electromagnetic energy dissipation function,  $L$  represents the Lagrange function, and its expression is:

$$L = T(q_j, \dot{q}_j) - V(q_j) + W_m(q_j, \dot{e}_k) - W_p(q_j, e_k) \quad (11)$$



In the formula,  $T$  represents the kinetic energy of Metro machinery,  $V$  represents the potential energy of Metro machinery,  $W_m$  represents the magnetic field energy of metro, and  $W_p$  represents the electric field energy of Metro.

The expression of dissipation function  $F_w$  can be written as:

$$F_w = F_m(q_j, \dot{q}_j) + F_p(\dot{e}_k) \quad (12)$$

In the formula,  $F_m$  represents the dissipation function of mechanical system and  $F_p$  represents the dissipation function of electromagnetic system.

Assuming that the overall mass of the metro is  $M$ , the moment of inertia of the wheel and the main shaft is  $J$ , the wheel radius is  $R$ , the displacement of the linear motor is  $x$ , and the rotation angle of the main shaft is  $\varphi$ , the Metro kinetic energy expression as shown in formula (13) can be constructed:

$$E_{k1} = \frac{1}{2}M \cdot \dot{x}^2 + \frac{1}{2}J \cdot \dot{\varphi}^2 \quad (13)$$

And the electromagnetic energy expression of Metro is constructed:

$$\begin{aligned} E_{k2} = & \frac{1}{2}i_{abc1}^T \cdot L_{S1} \cdot i_{abc1} + i_{abc1}^T \cdot \psi_{abc1} \\ & + \cdots + \frac{1}{2}i_{abcn}^T \cdot L_{Sn} \cdot i_{abcn} + i_{abcn}^T \cdot \psi_{abcn} \end{aligned} \quad (14)$$

In the formula,  $i_{abcn}$  represents the current of the linear motor,  $L_{Sn}$  represents the inductance of the linear motor, and  $L_{Sn}$  represents the flux linkage of the linear motor.

Add formula (13) and formula (14) to obtain a new Lagrange function expression:

$$L = E_{k1} + E_{k2} \quad (15)$$

Thus, a new expression of dissipation function  $F_w$  can be constructed:

$$\begin{aligned} F_w = & \frac{1}{2}i_{abc1}^T \cdot R_{S1} \cdot i_{abc1} + \cdots + \frac{1}{2}i_{abcn}^T \cdot R_{Sn} \cdot i_{abcn} \\ & + \frac{1}{2}D \cdot \dot{x}_1^2 + \cdots + \frac{1}{2}D \cdot \dot{x}_n^2 \end{aligned} \quad (16)$$

In the formula,  $D$  represents the viscous friction coefficient and  $R_{Sn}$  represents the energy consumption resistance of the linear motor.

In the process of studying the dynamics of linear metro, the influence of inertia needs to be considered. Therefore, a dynamic model is built in the

inertial coordinate system to study the dynamic performance of Metro. The dynamic model is built according to the operation parameters of linear metro, so it can simulate the operation characteristics of linear metro under different working conditions, and can get more accurate dynamic characteristic analysis results. The vector expression of any wear position in the elastic coordinate system is:

$$r_k^0 = r_{01}^0 + A_{01}^0(\rho_k^1 + d_k^1) \quad (17)$$

In the formula,  $r_{01}^0$  represents the path from the origin of the elastic coordinate system to the origin of the inertial coordinate system,  $A_{01}^0$  represents the conversion matrix,  $\rho_k^1$  represents the path from the location point  $K$  to the elastic coordinate system, and  $d_k^1$  represents the elastic displacement of the location point  $K$ .

Based on the above calculation results, the expression of linear motor position can be constructed by modal superposition method:

$$x = \sum_{j=1}^H h_j w_j = Hw \quad (18)$$

In the formula,  $H$  represents the modal matrix,  $h_j$  represents the modal value, and  $w_j$  represents the modal coordinates.

Combined with the elastic matrix, the expression of stress and strain is constructed:

$$\varepsilon = Dx_k \quad (19)$$

$$\sigma_k = H\varepsilon = HDx_k \quad (20)$$

In the formula,  $D$  represents the elasticity matrix.

Combining formula (17) to formula (20), the dynamic equation of linear metro can be constructed:

$$\begin{aligned} & \begin{bmatrix} mI & \dot{d}_{CM} & C_t \\ \ddot{d}_{CM} & J & C_r \\ C_t & C_r & M_e \end{bmatrix} \begin{Bmatrix} a \\ \dot{\omega} \\ \ddot{q} \end{Bmatrix} + \begin{bmatrix} m\tilde{\omega}\tilde{\omega}\dot{d}_{CM} \\ \tilde{\omega}I\tilde{\omega} + G_r\omega \\ O_e\Omega + G_e\omega \end{bmatrix} + \begin{Bmatrix} 0 \\ 0 \\ K_eq \end{Bmatrix} \\ & = \begin{bmatrix} \sum_k p_k \\ \sum_k \tilde{c}_k p_k \\ \sum_k X^T(c_k) p_k \end{bmatrix} \quad (21) \end{aligned}$$

In the formula,  $C_t$  represents the translational deformation coupling matrix,  $C_r$  represents the rotational deformation coupling matrix,  $d_{CM}$  represents the position of the deformation point,  $G_r$  represents the rotational force,  $G_e$  represents the rotational force,  $G_c$  represents the centrifugal force,  $a$  represents the acceleration, and  $\tilde{\omega}$  represents the vector machine.

## 5 Experimental Verification

In order to verify the performance of the proposed method, comparative experiments are carried out. First, it is necessary to build the dynamic model of the subway, as shown in Figure 7.

In Figure 7, the car body, structure, motor and gear transmission structure of the metro are rigid bodies with multiple degrees of freedom. As the subway lines in different cities are different, they can be set under the S-shaped curve in order to simulate different operating environments.

Parameters of linear metro are shown in Table 1.

The parameters of linear motor are shown in Table 2.

Relevant parameters of air resistance during metro operation of linear motor are shown in Table 3.

After setting the relevant parameters of the linear metro, collect the wear data of the metro. Since the obvious wheel rail wear only occurs under long-time and long mileage operation, the wheel rail wear data at 30000 km, 60000 km and 90000 km are selected respectively, as shown in Figure 8.

Based on the wheel rail wear data of linear motor Metro shown in Figure 8, experiments on wear prediction accuracy, stability and derailment coefficient are carried out to clarify the prediction performance and dynamic

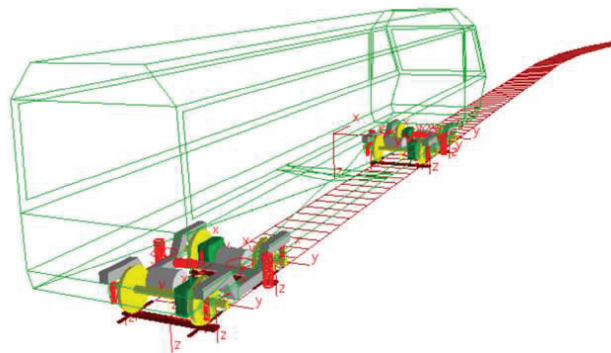


Figure 7 Linear metro dynamic model.

**Table 1** Metro parameters of linear motor

| Project                                     | Parameter             |
|---|-----------------------|
| Locomotive quality                          | 14900 kg              |
| Rotational inertia of wheel and main shaft  | 400 kg·m <sup>2</sup> |
| Wheel radius                                | 365 mm                |
| Supply voltage                              | DC1500V               |
| Friction coefficient between wheel and rail | 0.08                  |
| Vehicle length                              | 17 m                  |
| Vehicle width                               | 2.89                  |
| Vehicle height                              | 3.625                 |

**Table 2** Linear motor parameters

| Project                      | Parameter |
|------------------------------|-----------|
| Polar logarithm              | 12        |
| Electrical time constant     | 21.9      |
| Viscous friction coefficient | 1.2 Ns/m  |
| Effective flux linkage       | 0.607 wb  |
| Mover inductance             | 33 mH     |
| Armature resistance          | 1.5Ω      |
| Continuous thrust            | 5341 N    |
| Maximum thrust               | 12726 N   |
| Polar distance               | 0.032 m   |

**Table 3** Relevant parameters of air resistance

| Project                            | Parameter             |
|------------------------------------|-----------------------|
| Hydraulic diameter                 | 4.086 m               |
| Comprehensive hydraulics           | 1.2 kg/m <sup>3</sup> |
| Air hydraulic friction coefficient | 0.0116                |
| Aerodynamic drag coefficient       | 0.0525                |
| Cross sectional area of vehicle    | 10.476 m <sup>2</sup> |

research performance of the method, so as to comprehensively ensure the safety of linear motor metro operation.

### 5.1 Prediction Accuracy of Wheel Rail Wear

Since the safety of linear motor metro operation is directly related to the wear amount, if the wear amount can be accurately predicted, reasonable maintenance and replacement measures can be formulated according to the wear degree under different operating mileage or time, so as to improve the safety of metro operation. Therefore, in order to verify the performance of this

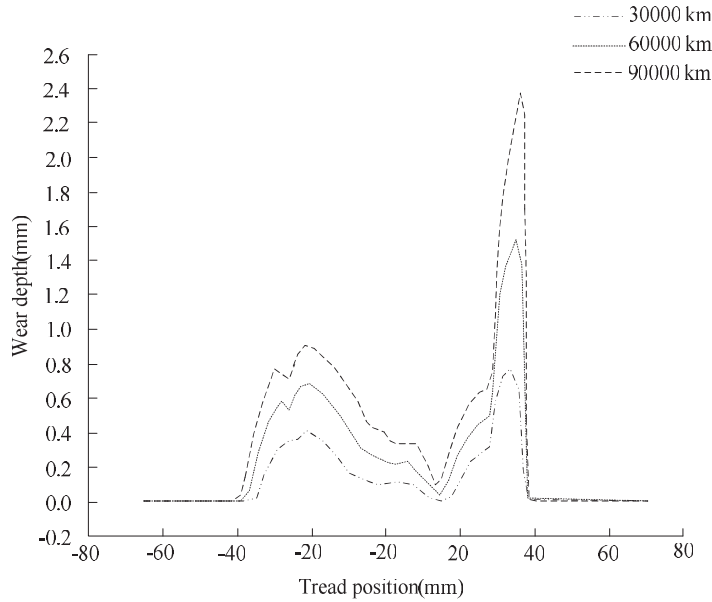


Figure 8 Wheel rail wear data.

method, this method is directly compared with reference [7] and reference [8] methods by taking the prediction accuracy of Metro wheel rail wear as the comparison index. The experimental results of prediction accuracy of Metro wheel rail wear are shown in Figure 9.

From the prediction accuracy results of Metro wheel rail wear shown in Figure 9, it can be seen that under different experiments, the prediction accuracy of this method is higher than that of the two comparison methods. Compared with the methods in reference [7] and reference [8], the prediction accuracy of Metro wheel rail wear of this method is above 97%, and the prediction accuracy of the highest wear is even 99%. However, the wear prediction accuracy of the methods in reference [7] and reference [8] does not exceed 90% at most. Therefore, it fully shows that this method can accurately predict the wheel rail wear of linear motor Metro and improve the safety of metro operation.

## 5.2 Stationarity

When analyzing the dynamic performance of linear motor metro operation, it is necessary to consider the stability index. In the study of subway operation

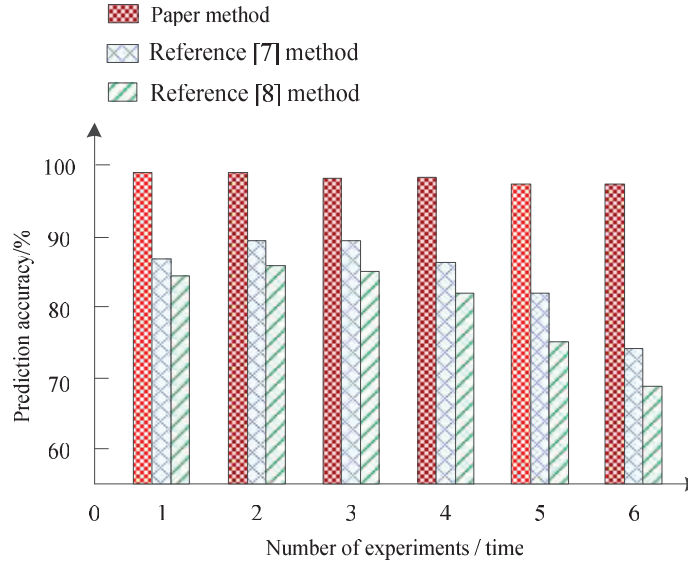


**Figure 9** Prediction accuracy of Metro wheel rail wear.

**Table 4** Vibration frequency correction factor

| Transverse Vibration |                 | Vertical Vibration |                   |
|----------------------|-----------------|--------------------|-------------------|
| 0.5~5.4 Hz           | $F(f) = 0.8f^2$ | 0.55.9 Hz          | $F(f) = 0.325f^2$ |
| 5.4~26 Hz            | $F(f) = 650f^2$ | 5.9~20 Hz          | $F(f) = 400f^2$   |
| >26 Hz               | $F(f) = 1$      | >20 Hz             |                   |

stability, the main factors considered are vibration frequency and vibration acceleration. Therefore, the calculation formula of Metro stability index can be established:

$$W = 7.08^{10} \sqrt{\frac{A^3}{f} F(f)} \tag{22}$$

In the formula,  $f$  represents the vibration frequency of the subway during operation,  $A$  represents the vibration acceleration of the subway, and  $F(f)$  represents the frequency correction factor. The value of frequency correction factor is shown in Table 4.

According to the above results, the stability of subway operation can be judged. The stability judgment results of linear metro are shown in Table 5.

Referring to the above calculation formula and stability index grade, considering that the maximum mileage in the collected data is 90000 km,

**Table 5** Level of Metro stability index

| Metro Stability Level | Metro Stability Grade Index | Assessment Results |
|-----------------------|-----------------------------|--------------------|
| Level 1               | <2.50                       | Excellent          |
| Level 2               | 2.50~2.75                   | Good               |
| Level 3               | 2.75~3.00                   | Qualified          |

**Table 6** Evaluation standard for derailment coefficient

| Evaluate | TB/T2360-1993 |      |           | GB5500-1895 |              |
|----------|---------------|------|-----------|-------------|--------------|
|          | Excellent     | Good | Qualified | First limit | Second limit |
| Q/P      | 0.6           | 0.8  | 0.9       | ≤1.2        | ≤1.0         |

it is not necessary to consider the stability at 30000 km and 60000 km, but only at 90000 km. The results of stationarity and initial values at 90000 km are shown in Figure 10.

By observing the running stability results of the linear metro shown in Figure 10, it can be seen that the stability of the wheel rail of the linear metro is basically consistent with the initial value, whether it is horizontal stability or vertical stability. Even after driving 90000 km, the stability of the linear metro remains at a good level, indicating that the safety of the metro operation has been improved to a certain extent.

### 5.3 Derailment Coefficient

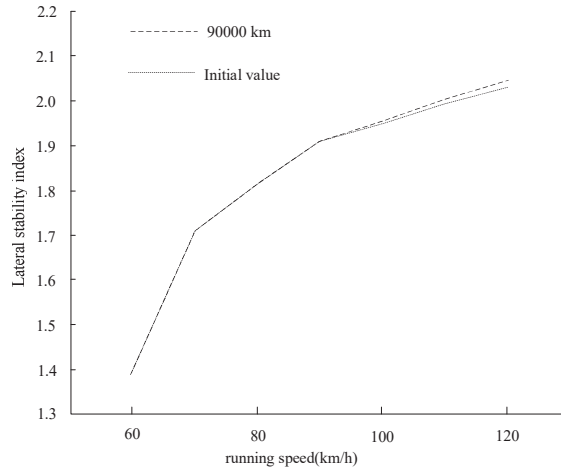
Derailment refers to that the subway is running off the track. Once a derailment accident occurs, it will directly damage the passengers and produce serious adverse effects. Therefore, it is necessary to study the derailment of linear motor Metro. In the process of derailment research, the ratio of wheel rail vertical force to lateral force is the key factor. The ratio of the two forces is the derailment coefficient, and the expression is:

$$\frac{Q}{P} = \frac{\sin \alpha - \eta \cos \alpha}{\eta \sin \alpha + \cos \alpha} \tag{23}$$

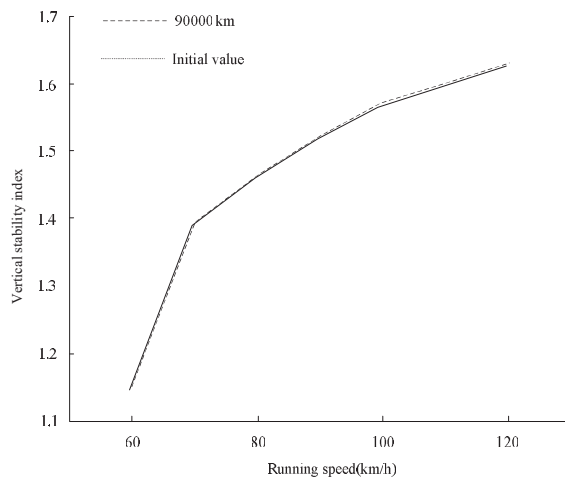
In the formula,  $\eta$  represents the wheel rail friction coefficient,  $\alpha$  represents the wheel flange angle,  $P$  represents the wheel rail vertical force, and  $Q$  represents the wheel rail lateral force.

The evaluation criteria for derailment coefficient during metro operation of linear motor are shown in Table 6.

According to the evaluation standard of derailment coefficient and the data collected by linear metro, only the derailment coefficient under



(a) Lateral stability index



(b) Vertical stability index

**Figure 10** Running stability results of linear motor Metro.

90000 km is considered. The derailment coefficient results of linear metro are shown in Figure 11.

From the results of derailment coefficient of linear metro shown in Figure 11, it can be seen that compared with the derailment coefficient under the initial plane, the derailment coefficient increases significantly when



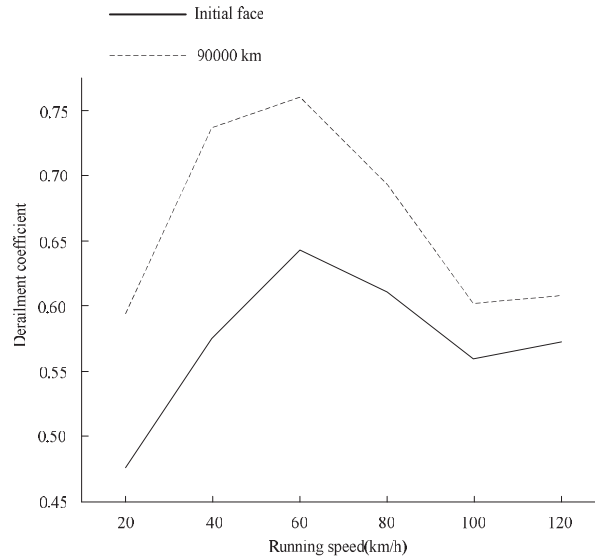


**Figure 11** Derailment coefficient results.

traveling for 90000 km, especially when the running speed of the metro is greatly 60 km/h, and the derailment coefficient reaches the maximum, which indicates that the possibility of derailment of linear metro is increased at this time, and the Metro staff should pay attention to the driving safety at this speed. From the above results, it can be seen that calculating the derailment coefficient of linear metro can effectively determine whether the running speed is safe under the driving mileage, so it provides a guarantee for improving the operation safety of linear metro.

To sum up, this study analyzes the friction characteristics between wheels and rails according to the working principle of linear motor. The MiniProf series profilometer is used to accurately collect the running data of the subway, calculate the wear energy flow density and the wear mass flow density of the wheel rail contact surface according to the collected data, and complete the wear prediction. According to the mechanical resistance and aerodynamic resistance, the modal superposition method is used to accurately calculate the position of linear power. According to the operating characteristic parameters, a dynamic model is built to clarify the dynamic performance of the subway. Through the performance test results of the existing methods, it can be seen that this method can accurately predict the wear of linear electric metro, and analyze the operation stability of linear electric Metro.

## 6 Conclusion

Aiming at the stability and safety of linear motor metro operation, this study proposes the prediction of wheel rail wear and dynamic performance analysis of linear motor Metro. The performance of the method is verified from both theoretical and experimental aspects. This method has high wear prediction accuracy and stability, derailment coefficient accuracy when carrying out linear motor Metro wheel rail wear prediction and dynamic performance analysis. Specifically, compared with the dynamic response performance research method proposed in reference [7] and the dynamic simulation model method proposed in reference [8], the prediction accuracy of wheel rail wear of this method is significantly improved, reaching more than 97%. And this method can accurately calculate the derailment coefficient of subway under different speeds. Therefore, it can better ensure the operation safety of linear metro.

## References

- [1] Pradhan S , Samanta B , Samantaray A K . Influence of active steering with adaptive control law on a metro rail vehicle wheel wear and dynamic performance[J]. *Journal of Mechanical Science and Technology*, 2020, 34(4):1415–1428.
- [2] Pradhan, Smitirupa, Samantaray, et al. A Recursive Wheel Wear and Vehicle Dynamic Performance Evolution Computational Model for Rail Vehicles with Tread Brakes[J]. *Vehicles*, 2019.
- [3] Shi Y , Dai H , Wang Q , et al. Research on Low-Frequency Swaying Mechanism of Metro Vehicles Based on Wheel-Rail Relationship[J]. *Shock and Vibration*, 2020, 2020(12):1–15.
- [4] Yin B . Dynamic Modeling and Simulation of Metro Wheel Wear Based on Cellular Automata Method[J]. *Journal of Mechanical Engineering*, 2019, 55(2):135.
- [5] Smitirupa P , Samantaray A K , Bhattacharyya R . Multi-step wear evolution simulation method for the prediction of rail wheel wear and vehicle dynamic performance[J]. *Simulation: Transactions of The Society for Modeling and Simulation International*, 2019, 95:441–159.
- [6] Liu Q , Lei X , Rose J G , et al. Vertical wheel-rail force waveform identification using wavenumber domain method[J]. *Mechanical Systems and Signal Processing*, 2021, 159(8):107784.

- [7] Zang Chuazhen, Wei Qingchao, Nie Xinlu. Dynamic response of the LIM wheel/rail train in curved section[J]. *Journal of Harbin Institute of Technology*, 2019, 51(9):7–10.
- [8] Huan Dong, Tao Gongquan, Xie Qinglin, et al. Influence of Hollow-Worn Wheels on Wheel-Rail Contact and Dynamic Performance of Metro Vehicle[J]. *Machinery*, 2021, 48(7):9–12.
- [9] Liu Wei, Zhang Xiongfei, Zhang Dongmei, et al. Experimental Investigation of Wear Characteristic and Dynamic Performance of Linear Metro Vehicles[J]. *Machinery*, 2020, 47(4):7–13.
- [10] Pradhan S , Samantaray A K . A Recursive Wheel Wear and Vehicle Dynamic Performance Evolution Computational Model for Rail Vehicles with Tread Brakes[J]. *Vehicles*, 2019, 1(1):88–114.
- [11] Zhang M , Li X , Liu X . Dynamic performance analysis of a urban rail vehicle based on rigid-flexible coupling[C]// AIP Conference Proceedings. AIP Publishing LLC AIP Publishing, 2019.
- [12] Jincheng L I , Ding J , Yang Y , et al. Research on Dynamic Performance and Wheel Damage of Metro Vehicle with Radial Bogie[J]. *Electric Drive for Locomotives*, 2019.
- [13] Kowalik R . Mechanical Wear Contact between the Wheel and Rail on a Turnout with Variable Stiffness[J]. *Energies*, 2021, 14.
- [14] Li H X , Zhu A H , Ma C C , et al. Influence of Wheel Profile Wear Coupled with Wheel Diameter Difference on the Dynamic Performance of Subway Vehicles[J]. *Shock and Vibration*, 2021.
- [15] Ye Y , Sun Y . Reducing wheel wear from the perspective of rail track layout optimization:[J]. *Proceedings of the Institution of Mechanical Engineers, Part K: Journal of Multi-body Dynamics*, 2021, 235(2): 217–234.
- [16] Chang C , Ling L , Han Z , et al. High-Speed Train-Track-Bridge Dynamic Interaction considering Wheel-Rail Contact Nonlinearity due to Wheel Hollow Wear[J]. *Shock and Vibration*, 2019, 2019:1–18.
- [17] Jiang Y P , Chi M R , Zhu H Y . Effects of Lateral Damper Invalid at Different Location on the Dynamic Performance of Metro Vehicle[J]. *Science Technology and Engineering*, 2019.
- [18] Chu Min, Li Xiaobo, Wang Ruiyi, Wang Quan. Reliability Prediction of Metro Traction Inverter System Based on Grey Optimization[J]. *Computer Simulation*, 2020, 37(07):168–171.
- [19] Shi J , Gao Y , Long X , et al. Optimizing rail profiles to improve metro vehicle-rail dynamic performance considering worn wheel profiles and

- curved tracks[J]. *Structural and Multidisciplinary Optimization*, 2021, 63(9).
- [20] Pradhan S , Samantaray A K , Bhattacharyya R . Multi-step wear evolution simulation method for the prediction of rail wheel wear and vehicle dynamic performance[J]. *SIMULATION: Transactions of The Society for Modeling and Simulation International*, 2019, 95(5):441–159.
- [21] Wei L , Tian L , Zheng J , et al. Evaluation of the Effect of Stray Current Collection System in DC-Electrified Railway System[J]. *IEEE Transactions on Vehicular Technology*, 2021, 70(7):89–96.
- [22] Sajeev. R , Chandramohan S . Analysis of Critical Hunting Speed and Running Safety of Conventional Railway Vehicle Truck on Curved Track[J]. *International Journal of Heavy Vehicle Systems*, 2021, 28(6):808–815.
- [23] Sebastian Stichel, Rickard Persson, Rocco Giossi. Improving Rail Vehicle Dynamic Performance with Active Suspension[C]//Abstracts of the 8th International Conference on Vibration Engineering (ICVE 2021), 2021:224.

## Biographies



**Ding Feng**, male, born in November 1970, professor of engineering, graduated from Dalian Railway Institute in 1992, majored in Machinery Manufacturing Technology, and is currently party branch secretary and vice minister of quality Assurance Department of Dalian Locomotive and Rolling Stock Co., Ltd. He has been engaged in the design and development of locomotives and urban rail vehicles for nearly 30 years. He has successively completed nearly 30 projects, such as the braking system design of “Dongfeng” series diesel locomotives, A and B Series subway vehicles, modern trams, intercity (urban) trains, medium speed and low speed maglev vehicles, etc., and has achieved three national key projects.



**Long Chen** is a student at Dalian Jiaotong University since 2006, electrical engineering and the automatization specialty, received master's degree in 2013. Long Chen works in CRRC Dalian Locomotive & Rolling Stock Co., Ltd., serving as designer and senior engineer, won a number of science and technology awards of CRRC Corporation and Liaoning Province.



**Yanxia Yu** works in CRRC Dalian Locomotive & Rolling Stock Co., Ltd., serving as chief designer and professoral-level senior engineer. Engage in the research and development and application of intelligent control products and train network control system, undertake the research and development of many major and key science and technology projects of China level and CRRC Corporation, and win a number of science and technology awards of CRRC Corporation and Liaoning Province.



**Yunfeng Zeng** graduated from Yanshan University, China in 2008 with a master's degree in control theory and control engineering. Yunfeng Zeng is a senior engineer, mainly engaged in the integrated design of train control system and the development of intelligent operation and maintenance. Since 2008, Yunfeng Zeng has been working as the designer of train control system in CRRC Dalian Co., LTD. He has won the science and technology award of CRRC and Dalian for many times, and has accumulated rich experience in the integrated design of train control system.